Journal of Molecular Liquids

Inclusion complexes of nabumetone with β-cyclodextrins: spectroscopic, spectrometric and calorimetric studies in different solvents

--Manuscript Draft--

Manuscript Number:	MOLLIQ-D-23-07686
Article Type:	Full length article
Section/Category:	Water, aqueous solutions and other hydrogen-bonded liquids
Keywords:	nabumetone; cyclodextrins; spectrofluorimetry; NMR spectroscopy; microcalorimetry; thermodynamic parameters
Corresponding Author:	Nives Galic University of Zagreb Faculty of Science Zagreb, CROATIA
First Author:	David Klarić
Order of Authors:	David Klarić
	Melita Kelrajter
	Ana Čikoš
	Ana Budimir
	Nives Galic
Abstract:	Complexation of nabumetone (NAB) with β-cyclodextrin (β-CD) and its derivatives, namely hydroxypropyl-β-CD (HPβCD), randomly methylated β-CD (RMβCD), and sulfobutylether sodium salt β-CD (SBEβCD) was investigated in detail. Increased solubility of NAB in water and in simulated biorelevant media (pH = 1.0 (HCl) and pH = 4.5 and 6.8 (phosphate buffer)) was achieved in the presence of all β-CDs, reaching approximately 170 times for SBβCD. Based on the phase-solubility measurements, complexation efficiency and stability constants for 1:1 complexes were calculated, and further confirmed by spectrofluorimetric titrations. The complex stoichiometry was additionally verified by high-resolution mass spectrometry. Thermodynamic parameters (lgK, ΔrG0, ΔrH0, ΔrS0) were determined by isothermal microcalorimetric titrations. The stability constants agree well with those obtained from fluorescence measurements (lgK = 3.42; 3.41; 3.47 and 3.62 for NAB complexes with β-CD, HPβCD, RMβCD, and SBβCD, respectively). The inclusion was enthalpy and entropy favorable and the mode of inclusion was determined by NMR spectroscopy. Complexation of approximately 20 % was observed in DMSO-d6, in contrast to essentially complete in deuterated water (ca 97 %). Two possible orientations of NAB in β-CD cavity simultaneously exist in the solution, with a naphthalene ring inside the β-CD cavity and methoxy or butanone substituent oriented towards the narrow β-CD rim. In addition, the formation of a hydrogen bond between the 6-CH2OH group in β-CD and the carbonyl group in NAB was observed. All experimental results are in good agreement with those based on molecular modeling previously reported in the literature.
Suggested Reviewers:	Janez Plavec, prof janez.plavec@ki.si expert in NMR spectroscopy
	Zoltan Aigner, prof aigner.zoltan@szte.hu specialist in pharmaceutical technology
	Luis Fernando Cabeça, prof luiscabeca@utfpr.edu.br preparation and characterization of inclusion complexes with beta-cyclodextrins and its derivatives
	Beatrice Perisutti, prof bperissutti@units.it

Powered by Editorial Manager® and ProduXion Manager® from Aries Systems Corporation

	preparation and characterization of new drug formulations
	Christian Schonbeck jechsc@ruc.dk solubility studies and stability constants determination of inclusion complexes with beta-cyclodextrins and its derivatives
Opposed Reviewers:	

Dear Editor,

We would like to submit our manuscript entitled ″Inclusion complexes of nabumetone with β-cyclodextrins: spectroscopic, spectrometric and calorimetric studies in different solvents″ and would very much appreciate if you would consider the manuscript for publication in *Journal of Molecular Liquids*.

Nabumetone (NAB) is a nonsteroidal anti-inflammatory prodrug used clinically to reduce pain and inflammation in the treatment of patients with osteoarthritis or rheumatoid arthritis. The main drawback of NAB is related to its poor water solubility, which can be efficiently addressed by inclusion complexation with cyclodextrins (CD). Both natural and chemical modified CDs are known to act as multifunctional excipients which enhance *in vitro* dissolution properties of drugs by changing their chemical and physical properties and thereby provide alternative ways of drug delivery.

To the best of our knowledge, there is only one paper describing the phase-solubility study of NAB in aqueous solution upon the addition of α- and γ-CD. Since no phase-solubility data for the NAB/β-CD system can be found in the literature, in this work we performed measurements with β-cyclodextrin (β-CD), 2-hydroxypropyl-β-cyclodextrin (HPβCD), randomly methylated β-cyclodextrin (RMβCD) and sulfobutylether sodium salt β-cyclodextrin (SBEβCD) in unbuffered aqueous solution, as well as in simulated biorelevant media at pH = 1.0, 4.5, and 6.8, to investigate the influence of HCl and phosphate buffer on solubilization. UV-Vis and spectrofluorimetric methods previously developed and validated by us were used for NAB determination in solution.

The interpretation of the NAB/β-CD inclusion phenomenon in literature is mainly based on molecular modeling studies while few experimental data are available. Therefore, we have conducted a comprehensive study of NAB inclusion interactions with β-CD, and its derivatives (RMβCD, HPβCD, SBEβCD) in solution, using various experimental techniques such as LC, HRMS, and NMR. NMR results suggested two possible orientations of NAB in the β-CD cavity and the simultaneous existence of both inclusion orientations in solution. In both the naphthalene ring sits in the hydrophobic cavity of the β-CD, while the substituents (methoxy and butanone) are oriented toward the edges of the cavity and point toward the solvent. This is the first experimental evidence of such equilibrium in solution. In addition to above mentioned techniques,

microcalorimetry titrations were employed to determine thermodynamic parameters (K, $\Delta_r H$, $\Delta_r S$, $\Delta_r G$) for drug-CDs systems.

The results of different methods applied were in accordance. In addition, all findings acquired by experimental methods were in excellent agreement with those previously suggested on *in silico* results. In our opinion the manuscript fits well in the scope of *Journal of Molecular Liquids*.

We confirm that this manuscript has not been published elsewhere and is not under consideration by another journal. All authors have approved the manuscript and agree with submission to *Journal of Molecular Liquids*. We have read and accepted Ethical Guidelines to Publication of Chemical Research. The authors have not conflict to interest to declare.

Sincerely,

Nives Galić

ngalic@chem.pmf.hr

Highlights

- β-cyclodextrin derivatives increase nabumetone solubility in water and biorelevant media
- lg$K$, $\Delta_r G^0$, $\Delta_r H^0$ and $\Delta_r S^0$ were determined by isothermal microcalorimetric titrations
- The mode of inclusion was determined by NMR spectroscopy
- Two possible orientation of drug in β-CD cavity simultaneously exist in solution
- Complexation in DMSO and water was *ca* 20% and 97% respectively

Graphical Abstract

Click here to access/download;Graphical Abstract;Graphical abstract.tif

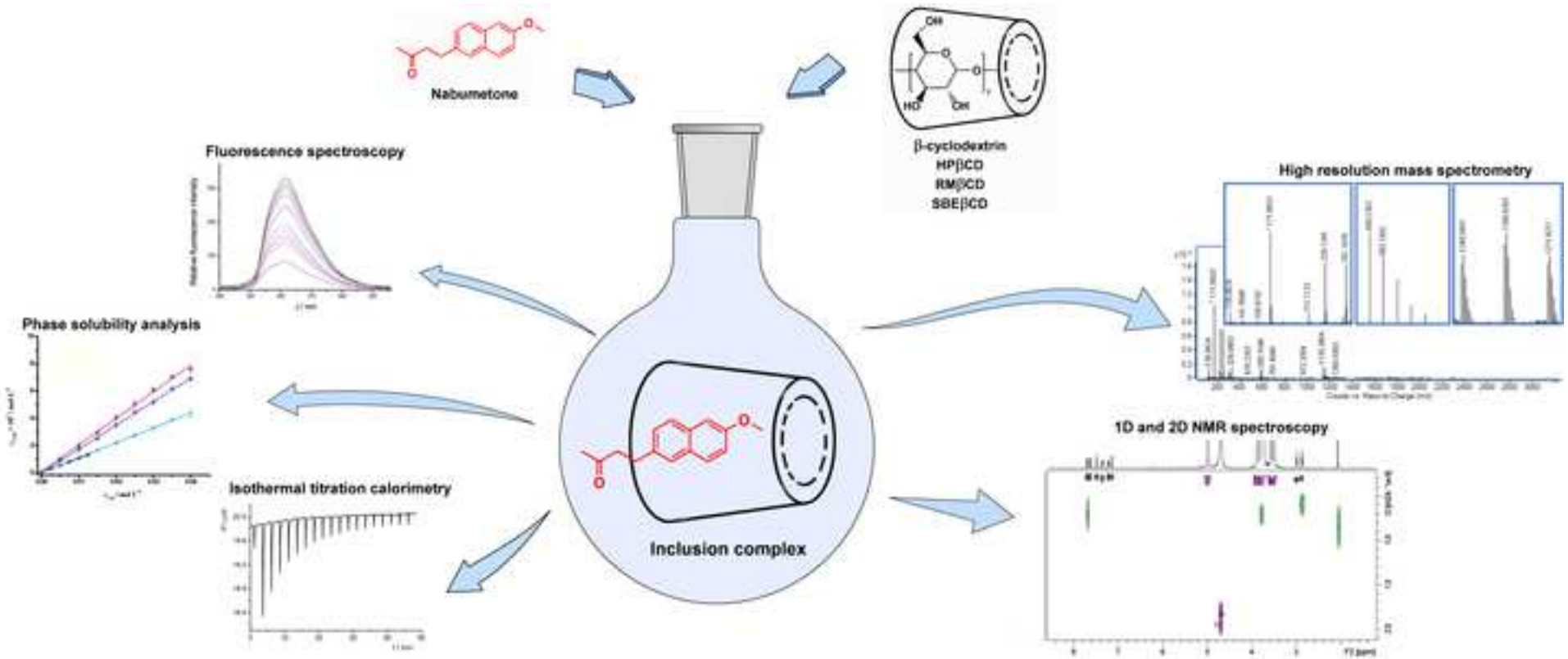

Manuscript File Click here to view linked References

Inclusion complexes of nabumetone with β-cyclodextrins: spectroscopic, spectrometric and calorimetric studies in different solvents

David Klarić,[1] Melita Kelrajter,[1] Ana Čikoš,[2] Ana Budimir[3] and Nives Galić[1*]

[1]Department of Chemistry, Faculty of Science, University of Zagreb, Horvatovac 102a, Zagreb Croatia

[2]Ruđer Bošković Institute, NMR Centre, Bijenička cesta 54, Zagreb, Croatia

[3]Department of General and Inorganic Chemistry, Faculty of Pharmacy and Biochemistry, University of Zagreb, A. Kovačića 1, Zagreb, Croatia

*Corresponding author: ngalic@chem.pmf.hr

Abstract

Complexation of nabumetone (NAB) with β-cyclodextrin (β-CD) and its derivatives, namely hydroxypropyl-β-CD (HPβCD), randomly methylated β-CD (RMβCD), and sulfobutylether sodium salt β-CD (SBEβCD) was investigated in detail. Increased solubility of NAB in water and in simulated biorelevant media (pH = 1.0 (HCl) and pH = 4.5 and 6.8 (phosphate buffer)) was achieved in the presence of all β-CDs, reaching approximately 170 times for SBβCD. Based on the phase-solubility measurements, complexation efficiency and stability constants for 1:1 complexes were calculated, and further confirmed by spectrofluorimetric titrations. The complex stoichiometry was additionally verified by high-resolution mass spectrometry. Thermodynamic parameters ($\lg K$, $\Delta_r G^0$, $\Delta_r H^0$, $\Delta_r S^0$) were determined by isothermal microcalorimetric titrations. The stability constants agree well with those obtained from fluorescence measurements ($\lg K$ = 3.42; 3.41; 3.47 and 3.62 for NAB complexes with β-CD, HPβCD, RMβCD, and SBβCD, respectively). The inclusion was enthalpy and entropy favorable and the mode of inclusion was determined by NMR spectroscopy. Complexation of approximately 20 % was observed in DMSO-d_6, in contrast to essentially complete in deuterated water (ca 97 %). Two possible orientations of NAB in β-CD cavity simultaneously exist in the solution, with a naphthalene ring inside the β-CD cavity and methoxy or butanone substituent oriented towards the narrow β-CD rim. In addition, the formation of a hydrogen bond between the 6-CH_2OH group in β-CD and the carbonyl group in NAB was observed. All experimental results are in good agreement with those based on molecular modeling previously reported in the literature.

Key-words: nabumetone, β-cyclodextrins, spectrofluorimetry, NMR spectroscopy, microcalorimetry, thermodynamic parameters

1. Introduction

Nabumetone (NAB) is a nonsteroidal anti-inflammatory prodrug used clinically to reduce pain and inflammation in the treatment of patients with osteoarthritis or rheumatoid arthritis [1]. NAB acts as a cyclooxygenase inhibitor after being metabolized in the liver to 6-methoxy-2-naphthylacetic acid. According to the Biopharmaceutical Classification System NAB is categorized as a class II drug, meaning it exhibits low aqueous solubility, and consequently low bioavailability [2]. To be pharmacologically effective, all drugs must be soluble in water to some extent, and most of them should be lipophilic to penetrate biological membranes. Various technologies and methods are continuously being developed aiming to improve solubility, such as solid dispersions, self-emulsifying drug delivery systems, nanocrystals, and drug inclusion into macrocycles such as cyclodextrins (CDs) [3,4]. Some of these techniques, such as nanostructured lipid carriers [2,5] have been used to enhance the solubility and improve the intestinal absorption of orally administered NAB. Inclusion of drugs into macrocycles such as cyclodextrins (CDs) remains a hot topic for development in the pharmaceutical industry because they can be used as drug delivery systems for poorly soluble compounds, for compounds that would otherwise be metabolized before reaching their target, or for modification of the drug administration mode [6–8].

Cyclodextrins are a group of cyclic oligosaccharides containing six (α-CD), seven (β-CD), or eight (γ-CD) D-glucopyranose units that are α-(1,4)-linked in a ring formation. Their structure presents as a truncated cone with a hydrophilic outer surface and a hydrophobic central cavity. Nowadays, CDs are used as drug carriers because they can improve the solubility and, therefore, bioavailability of poorly soluble drugs by taking up lipophilic drug moieties into their hydrophobic central cavity and forming water-soluble inclusion complexes [9–11]. Beside β-CD, hydroxypropyl-β-CD (HPβCD), sulfobutylether-β-CD (SBEβCD) and randomly methylated β-cyclodextrin (RMβCD) derivatives have gained pharmaceutical interest as they are also approved as pharmaceutical excipients [12–14].

The literature background shows that the interactions of NAB with naturally occurring CDs (α-CD, β-CD, γ-CD) and some β-CD derivatives were mostly studied by fluorescence spectroscopy [15–17], with thermodynamic parameters determined by the Van′t Hoff equation. In other examples, ^{1}H NMR was used to confirm the inclusion phenomena [15,16]. Having established that NAB forms complexes with β-CD, Valero *et al.* [15] concluded that NAB can adopt two orientations within the β-CD cavity. In the first (Fig. 1A), 6-methoxy protrudes through the narrow part of the β-CD, the naphthalene sits snugly within the cavity, and the 2-

butanone is exposed to the solvent through the wider part of the β-CD. In the second orientation (Fig. 1B) NAB is reversed, with the 6-methoxy facing the wide and 2-butanone the narrow part of the β-CD cavity. The observed proton NMR chemical shifts perturbation confirmed the inclusion, but there was no evidence of the preferred orientation. Moreover, NMR experiments were performed in the presence of ethanol which improved the solubility of NAB but may have altered the inclusion through competition with NAB. Goyenechea *et al*. [16] avoided ethanol in their NMR experiments and performed molecular mechanics calculations. Their modeling results suggest that both NAB orientations may be possible. The other studies on NAB/β-CD complexes relied mainly on modeling methods and their results converge on orientation A as being more favorable. Chen *et al*. postulate [18] that the methoxy group is pushed toward the narrow rim of the β-CD, while butanone does not interact with the host and rotates freely in the solution. Molecular dynamics results [19] show 40 % conformations with 2-butanone at the wide rim of the β-CD, where the hydrogen bond is formed between the carbonyl group and OH of the secondary alcohol in the β-CD (C=O···H_2O···HO-CH_2). Quantum chemical results [20] demonstrate that the inclusion of NAB in β-CD is a thermodynamically favorable process since both NAB conformations have negative complexation energy. Additionally, conformation A has –0.98 Kcal mol^{-1} lower energy than conformation B, making it a preferred conformation. The naphthalene moiety forms strong van der Waals interactions and weak intermolecular hydrogen bonds with the host cavity, while the 2-butanone group is at the wide rim, exposed to the solvent.

Therefore, the interpretation of the NAB/β-CD inclusion phenomenon is mainly based on molecular modeling studies [16, 18–20] while few experimental data are available. Therefore, we have conducted a comprehensive study of NAB inclusion interactions with β-CD, and its derivatives (RMβCD, HPβCD, SBEβCD) in solution, using various experimental techniques such as LC, NMR, and HRMS. In addition, microcalorimetry titrations were employed to determine thermodynamic parameters in water (K, $\Delta_r H$, $\Delta_r S$, $\Delta_r G$) and to investigate the extent to which the organic solvent may have influenced the inclusion phenomenon.

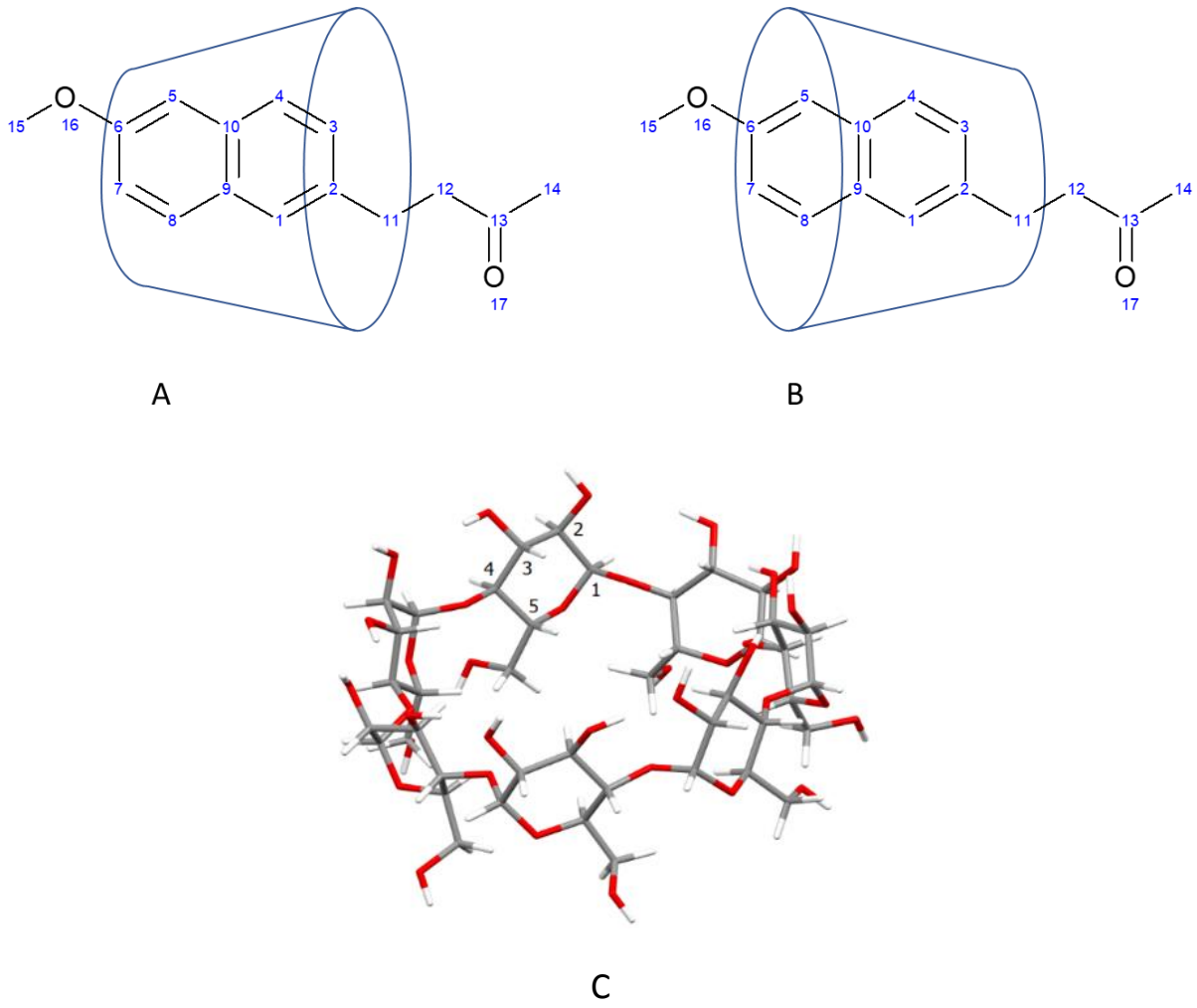

Fig. 1. Structures and numbering for two proposed orientations of nabumetone in β-cyclodextrin cavity (A and B), and crystal structure of β-cyclodextrin (C) [11,15].

2. Materials and methods

2.1. Materials

All chemicals were used as received without any further purification. Nabumetone (NAB) was purchased from Cayman Chemical (Ann Arbor, SAD). All cyclodextrins, β-cyclodextrin (β-CD), 2-hydroxypropyl-β-cyclodextrin (HPβCD, with an average degree of substitution, DS = 4.5), randomly methylated β-cyclodextrin (RMβCD, DS = 12) and sulfobutylether sodium salt β-cyclodextrin (SBEβCD, DS = 6.5) were obtained from CycloLab (Hungary). The solid 1:1 NAB: β-CD complex was prepared by grinding and analyzed by standard methods. LC-MS grade formic acid, acetonitrile, methanol, and DMSO (p.a.) were obtained from Carlo Erba.

Ultrapure water was obtained by Mili-Q Advantage A10 purification system (Merck). Deuterated solvents (DMSO-d_6 and D_2O) were purchased from Eurisotop (Cambridge Isotope Laboratories, Inc).

2.2. Instrumentation

For phase-solubility studies Tehtnica EV-402 and Tehtnica Vibromix 403 EVT orbital shakers were used.

UV-Vis measurements were carried out using a Specord 200 spectrophotometer (Analytik Jena AG, Germany). The absorption spectra were recorded in the spectral range from 200 nm to 400 nm in conventional quartz cells (l = 1 cm). The NAB absorbance was measured at 232 nm in 70:30 acetonitrile:water (ACN:H_2O)solution.

Emission spectra were recorded on a PerkinElmer Inc. LS55 spectrofluorimeter over the range of 300-450 nm. For phase solubility studies, measurements were performed in 70:30 ACN:H_2O solution (λ_{ex} = 315 nm, λ_{em} = 353 nm). Spectrofluorimetric titrations were carried out in 1:450 ACN:H_2O solutions to minimize the effect of ACN on complex formation (λ_{ex} = 262 nm, λ_{em} = 354 nm). Excitation and emission slit widths were amounted to 5 nm.

High-resolution mass spectra were acquired on an Agilent 6550 Series Accurate-Mass Quadrupole Time-of-Flight (Q-TOF). Solutions were introduced directly via an Agilent 1290 Infinity II UHPLC (flow injection analysis). The mobile phase was composed of 0.1% FA in MeOH (A) and 0.1% FA in H_2O in an isocratic mode 70:30 (*v*/*v*). The flow rate was set to 0.4 mL min^{-1} and the injection volume was 5 μL. The ESI–MS spectra were obtained in positive ion mode ranging from *m*/*z* 100 to *m*/*z* 3200. Fine-tuning of ESI ionization source parameters was performed to achieve higher abundances of complex ions in MS spectra. The capillary voltage was 3000 V, fragmentor voltage 350 V, drying gas flow 15 dm^3 min^{-1}, and temperature 225 °C. Sheath gas flow was 10 dm^3 min^{-1} and the temperature was 325 °C. The nozzle voltage was 1500 V. Nitrogen was used as a drying and sheath gas. For MS/MS spectra, the collision potential was varied from 10 to 40 V.

All NMR spectra were recorded at 25 °C using standard Bruker pulse sequences on Bruker Avance AV600 spectrometer equipped with room temperature 5 mm BBO probe with z-gradient accessory. The complete NMR analysis was based on one- and two-dimensional NMR spectra (^1H, ^{13}C, COSY, NOESY, 1D and 2D ROESY, DOSY, HSQCe and HMBC, Figs. S14-S40). The WaterGate scheme was used to suppress the HDO signal. NOESY spectra were obtained with a mixing time of 500 ms. The duration of the ROESY spinlock was 300 ms. The

data was processed using the Bruker TopSpin software package. The DOSY NMR spectra were acquired using dstebpgp3s, a pseudo 2D sequence using double stimulated echo for convection compensation and longitudinal encode-decode (LED) with bipolar gradient pulses for diffusion and three spoil gradients [21,22].

Due to the drastic difference in sample concentration, the spectra were acquired with 16 scans (DMSO-d_6), 32 scans (β-CD in D_2O), 256 scans (NAB/β-CD complex in D_2O), and 512 scans (NAB in D_2O) for each gradient step and the linear gradient was chosen in the range from 2 % to 95 %. The diffusion time (big delta, Δ) was 160 ms (DMSO-d_6) and 100 ms (D_2O), while the gradient duration (little delta, δ) was set to 2.1 ms (DMSO-d_6) and 1.5 ms (D_2O). The spectra were processed using Dynamics Center 2.6.3 software. The fitted function was:

$$f(x) = I_0 * e^{-D*\gamma^2*x^2*\delta^2*\left(\Delta-\frac{\delta}{3}\right)*10^4}$$

where γ is 26752 rad/(sG). I_0 represents the signal integral, and variable (x) is the gradient strength.

For microcalorimetric titrations, PEAQ-ITC MicroCal (Malvern Panalytical Ltd, UK) was used.

2.3. Phase solubility studies

Solubility measurements were performed according to Higuchi and Connors [23]. To each 10 mg NAB sample, the selected cyclodextrins were added. The final concentration of β-CD was in the range 0–12.5 × 10^{-3} mol L^{-1}, and for β-CD derivatives 0–40 × 10^{-3} mol L^{-1}. Suspensions were shaken at room temperature for 24, 48, and 72 h and filtered using 0.45 µm Chromafil Xtra H-PTFE filters (Macherey-Nagel, Germany). The NAB concentration in diluted samples was determined by previously developed and validated UV-Vis and spectrofluorimetric methods. The solubility diagrams were constructed, and stability constant ($K_{1:1}$) and complexation efficacy (*CE*) were calculated using the following formulas

$$K_{1:1} = \frac{slope}{S_0(1-slope)}$$

$$CE = \frac{slope}{1-slope}$$

where S_0 is the intrinsic solubility of a poorly soluble drug. The experiments were repeated three times in pure water, and one time in simulated biorelevant media. The buffer solutions were prepared according to European Pharmacopoeia [24], *e.g.* pH = 1 (HCl) and pH = 4.5 and 6.8 (phosphate buffer).

2.4. Spectrofluorimetric titrations

The titrations were performed as a batch to obtain the adequate NAB:β-CDs molar ratio. Each sample was prepared separately in a 5.0 mL flask by varying the β-CDs concentration (from 0 to 2.25×10^{-3} mol L^{-1}) while the concentration of NAB was kept constant (1×10^{-6} mol L^{-1}). The spectra were acquired one hour after the solutions preparation to ensure that complete equilibrium was reached. Titrations were repeated at least three times.

2.5. High-resolution mass spectrometry

Stock solutions of NAB and β-CDs were prepared in MeOH and H_2O, respectively. Solutions of complexes with various *n*(NAB):*n*(β-CD) molar ratios (1:1, 1:5, and 1:10) were prepared in methanol/water 1/1 mixtures. The final concentration of NAB in measured solutions was 4.40×10^{-5} mol L^{-1}.

2.6. Isothermal titration calorimetry

Microcalorimetric experiments were performed at 25.0 °C. All solutions were prepared in purified water (Milli-Q, Millipore) and briefly degassed before use. The reaction cell was filled with NAB solution (V_0 = 0.20 mL; $c_0 = 4.34 \times 10^{-5}$ mol L^{-1} or 4.89×10^{-5} mol L^{-1}), and enthalpy changes were recorded upon stepwise automatic addition of β-CDs solution (at 150 s intervals). The concentration of β-CDs in the stirrer syringe was more than 175 times higher than that of the NAB. The enthalpy changes measured were corrected for the enthalpy changes corresponding to the dilution of β-CDs obtained in the control experiments. The control experiments were performed for each titration experiment using the same ITC method and the same working solutions as for the complexation experiments. The enthalpy changes corresponding to both β-CD and NAB dilution by pure water were negligible. The dependence of the successive enthalpy changes on the titrant volume was analyzed using a single binding site model available in the analysis software MicroCal PEAQ-ITC (version 1.30). The stoichiometry was set to 1.00 in the fitting procedure because the binding affinities were low, and the binding stoichiometry was determined in separate experiments (sec. 2.3; 2.4; 2.5). All measurements were repeated three or more times.

2.7. NMR analysis

The samples for NMR analysis were prepared in DMSO-d_6 and D_2O. The final concentration of NAB, β-CD, and NAB/β-CD 1/1 complex in 600 μL of DMSO-d_6 was 35×10^{-3} mol L^{-1}. For NMR analysis in D_2O, 1.0 mg of NAB, 5 mg of β-CD, and 6 mg of NAB/β-CD 1/1 complex were each dissolved in 600 μL of D_2O to achieve the concentration of 7×10^{-3} mol L^{-1}. 600 μL of all three solutions were transferred to 5 mm NMR tubes, but almost all NAB and part of the complex precipitated. The exact final concentrations were not determined, the samples were recorded as is.

3. Results and discussion

3.1. Phase-solubility studies

To the best of our knowledge, there is only one paper describing the phase-solubility study of NAB in aqueous solution upon the addition of α- and γ-CD [25]. For NAB/α-CD system a non-linear plot with concave-upward curvature (A_P type) was observed, indicating the formation of 1:1 and 1:2 complexes. The constants were calculated to be 77.3 and 57.7 mol^{-1} L, respectively. On the other hand, for NAB/γ-CD system, the B_S type equilibrium and precipitation of an insoluble complex was observed. The calculated constant was 219 mol^{-1} L. The authors concluded that the α-CD cavity is too small to enclose NAB, while the large γ-CD forms weak interactions that would lead to premature release of the drug [25]. Since no phase-solubility data for the NAB/β-CD system can be found in the literature, in this work we performed measurements with β-CDs in unbuffered aqueous solution, as well as in simulated biorelevant media at pH = 1.0, 4.5, and 6.8, to investigate the influence of HCl and phosphate buffer on solubilization. The total NAB concentration was determined using in-house developed and validated UV-Vis and spectrofluorimetric methods (Supporting Information, SI, Table S1) after 24, 48, and 72 hours (SI, Fig. S1). All constructed phase diagrams were classified as A_L type (Figs. 2 and S2) indicating the formation of 1:1 NAB:β-CDs complexes [23]. The stability constants for β-CD, HPβCD, RMβCD and SBEβCD complexes with NAB and corresponding complexation efficiencies are given in Table 1. At this point, it should be mentioned that the equilibrium was reached within 24 h, and there was no significant difference in values measured after 24, 48, or 72 hours. The results suggest that all tested β-CDs improve NAB solubility. RMβCD and SBEβCD had the most significant effect, with an increase of up to ca. 160-170 fold. The phase solubility diagrams for NAB/β-CD and NAB/HPβCD systems overlap (Fig. 2), resulting in almost identical values for the corresponding stability constants. However, due to

the better solubility of HPβCD, the calculated S_{MAX}/S_0 value for this particular system is higher (Table 1). The use of HCl, as well as the phosphate buffer had no significant effect on the NAB solubility in the presence of the different β-CDs, as shown in Table S2.

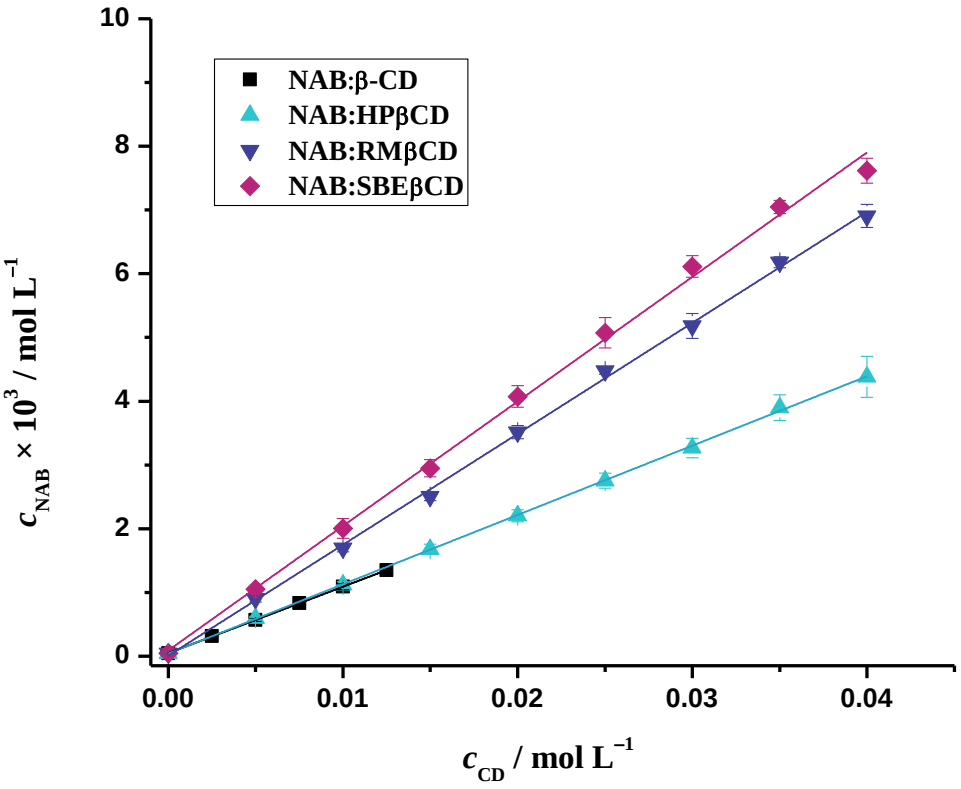

Fig. 2. Phase-solubility diagrams of NAB with β-CD(■), HPβCD(▲), RMβCD(▼) and SBEβCD(♦) in water at ambient temperature after 24 h obtained by UV-VIS method of quantification.

Table 1. Stability constants ($K_{1:1}$), complexation efficiencies (*CE*), and solubility enhancement (S_{MAX}/S_0) for complexes of NAB with selected β-CDs in water at ambient temperature after 24 h obtained by UV-Vis spectroscopy and spectrofluorimetry (number of measurements = 3)

		β-CD	HPβCD	RMβCD	SBEβCD
$K_{1:1}$ ± SE / M^{-1}	UV-Vis	2712.75 ± 284.86	2772.85 ± 255.54	4829.58 ± 191.90	5396.41 ± 445.74
	Fluor.	2629.81 ± 112.44	2597.81 ± 80.41	4655.02 ± 304.68	5105.27 ± 238.36
CE ± SE	UV-Vis	0.12 ± 0.01	0.12 ± 0.01	0.21 ± 0.01	0.24 ± 0.003
	Fluor.	0.12 ± 0.002	0.13 ± 0.01	0.23 ± 0.02	0.25 ± 0.02
S_{MAX}/S_0 ± SE	UV-Vis	31 ± 3	99 ± 7	158 ± 6	169 ± 15
	Fluor.	30 ± 1	93 ± 3	155 ± 13	166 ± 6

SE = standard error of the mean

3.2. Spectrofluorimetric titrations

To determine the stability constants (*K*) by phase solubility studies, the equation including the intrinsic solubility of a drug (S_0), defined as the intercept on the y-axis, was used. To eliminate possible errors due to extrapolation, spectrofluorimetric titrations were also performed. The increase in NAB emission upon the addition of spectrally inactive β-CDs was recorded in the spectral range from 300 nm to 450 nm. The obtained experimental results were fitted to a model involving only the formation of a 1:1 inclusion complex using the Specfit program. As an example, the dependence of the emission spectra of NAB on the β-CD concentration is shown in Fig. 3a. The plot of the measured and calculated fluorescence intensities is shown in Fig. 3b. The results of spectrofluorimetric titrations of NAB with the remaining CDs are available in the SI (Figs. S3-S5). The increase in NAB fluorescence intensities was observed for all β-CDs but is more pronounced for β-CD derivatives. Similar results were previously obtained by Goyenechea *et al*. [16]. The increase in NAB emission in NAB/β-CDs systems is related to inclusion phenomena causing changes in the solvation shell of NAB.

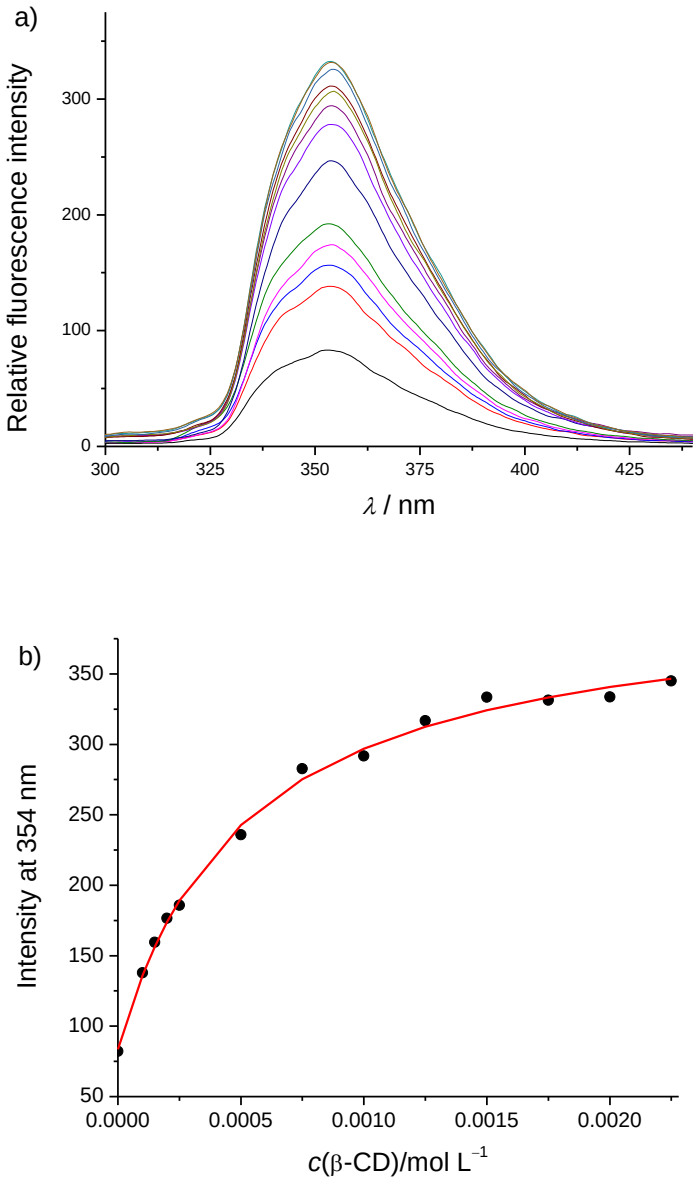

Fig. 3. a) Spectrofluorimetric titration of NAB (c = 1 × 10^{-6} mol L^{-1}) with β-CD in water. λ_{ex} = 262 nm; b) Dependence of fluorescence intensity at 354 nm on β-CD concentration. (●) experimental; (—) calculated.

The average formation constant values from three experiment sets are given in Table 2. The formation of 1:1 NAB/β-CDs complexes was additionally confirmed by applying the Benesi-Hildebrand linear regression method to determine K (Figs. S6-S9, Table S3) [26]. The constants are quite comparable to those previously reported for NAB/β-CD and NAB/HPβCD complexes determined by linear regression [15].

Table 2. Stability constants (lg*K*) for 1:1 complexes of NAB with selected β-CDs in water at ambient temperature determined by spectrofluorimetric titrations

Cyclodextrin	β-CD	HPβCD	RMβCD	SBEβCD
lg*K* ± SE	3.34 ± 0.04	3.28 ± 0.05	3.49 ± 0.04	3.62 ± 0.04

SE = standard error of the mean (N = 3)

3.3. High resolution mass spectrometry (HRMS)

ESI-MS represents a powerful method for the analysis of weakly bound non-covalent complexes. It can be used to determine the stoichiometry of host/guest complexes in the gas phase, which can be correlated with those in solutions [11]. In this work, solutions of NAB with β-CDs were studied by HRMS. Regardless of the changes in the NAB/β-CDs molar ratios, the composition of the mobile phase, and instrumental parameters settings, we were able to acquire only MS spectra of the NAB/β-CD complex (Fig. 4, Table S4). As can be seen, the base peak corresponds to the NAB fragment ion (*m/z* 171), a stable carbocation formed by β-cleavage adjacent to the carbonyl group. Further fragmentation leads to the naphthalene ion ($C_{10}H_8^{+\bullet}$, *m/z* 128.06). These *m/z* values were previously found during the LC-MS/MS analysis of pharmaceutical compounds in herbal food products and were assigned to NAB fragments [27]. Low intensity signals corresponding to doubly charged 1:1 ($[NAB+\beta\text{-CD}+Na+H]^{2+}$, *m/z* 693) and 1:2 complexes ($[NAB+2\beta\text{-CD}+2H]^{2+}$, $[NAB+2\beta\text{-CD}+Na+H]^{2+}$, $[NAB+2\beta\text{-CD}+2Na]^{2+}$, *m/z* 1249, 1260 and 1271 respectively) were present in MS spectra of solutions with equimolar NAB/β-CD ratio, as well as in the solutions with β-CD in excess. Since only 1:1 NAB:β-CD complexes have so far been observed in solution by spectroscopic methods, the formation of the 1:2 complex is probably a consequence of the electrospray process. The occurrence of $NAB(\beta\text{-CD})_2$ in solution was previously suggested in the form of a ternary complex where polymer polyvinylpyrrolidone acts as a bridge between two β-CD molecules binding the drug [28].

The β-CD derivatives (namely RMβCD, HPβCD, SBEβCD) have different degrees of substitution ranging from 4 to 14, which makes their MS spectra very complex, with a cluster of signals for each number of substituents on the β-CD molecule (Fig. S10). Taking into account the fact that the most intense signal in the MS spectrum originates from the in-source NAB fragment ion, the fact that drug complexes with β-CD derivatives are spread over all

cyclodextrin molecules, regardless of the degree of substitution, and that the ionization of the complexes is not very efficient, the signals from NAB complexes with β-CD derivatives were not observed in the corresponding MS spectra.

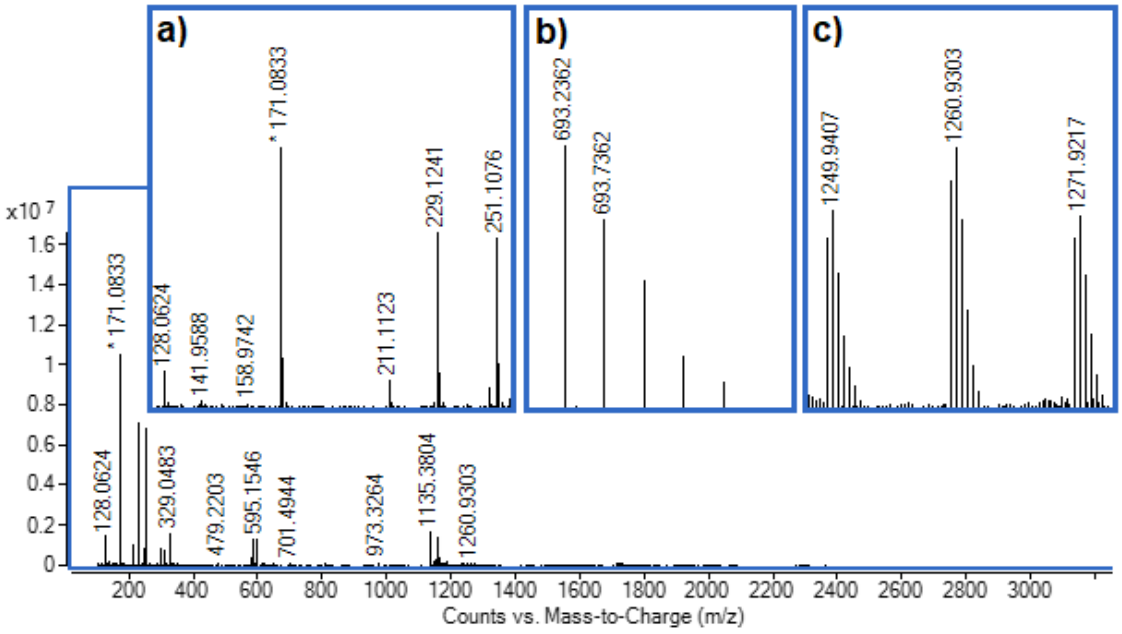

Fig. 4. HRMS spectrum of NAB and β-CD solution. The insets show the expanded region (signals of NAB, NABβ-CD and NAB(β-CD)$_2$ complexes).
c(NAB) = c(β-CD) = 4.40 × 10^{-5} mol L^{-1}

To gain more insight into NAB/β-CD complexes, the tandem MS analysis was performed. The intensity of the singly charged ions was not intensive enough to isolate an adequate *m/z* value, so MS/MS spectra of the doubly charged ions [NAB+β-CD+Na+H]$^{2+}$ (*m/z* 693.2362), [NAB+2β-CD+2H]$^{2+}$ (*m/z* 1249.4374), [NAB+2β-CD+Na+H]$^{2+}$ (*m/z* 1260.4285) and [NAB+2β-CD+2Na]$^{2+}$ (*m/z* 1271.4196) were acquired at different collision energies (10.0, 20.0, and 40.0 eV; Tables S5-S7). The MS/MS spectra of selected ions at 20 eV are shown in Fig. 5. As can be seen, the fragmentation patterns are similar for [NAB+2β-CD+2H]$^{2+}$ and [NAB+2β-CD+Na+H]$^{2+}$ ions, in both cases showing that complexes are cleaved, leaving the charge on one β-CD unit. In the case of the latter, the adducts with Na$^+$ ions, as well as protonated ions are formed, so two sets of signals are observed in the spectrum, including the [2β-CD+Na+H]$^{2+}$ ion (*m/z* 1146.3612). The [β-CD+H]$^+$ and [β-CD+Na]$^+$ ions are further cleaved by the successive loss of the glucopyranose unit resulting in ions with signals at *m/z* 973, 811, 649, 487, and very intensive one at *m/z* 325, assigned to two protonated units [29]. Interestingly, the

formation of $[\beta\text{-CD+H}]^+$ and $[\beta\text{-CD+Na}]^+$ adducts with one or more glucopyranose units is also observed, with corresponding signals at higher *m/z* values (1297, 1459, 1621, and 1319, 1481, 1643, respectively). However, the ion $[\beta\text{-CD+Na}]^+$ (*m/z* 1157) formed by cleavage of $[\text{NAB+2}\beta\text{-CD+2Na}]^{2+}$ is very stable, even at a higher collision energy of 40 eV.

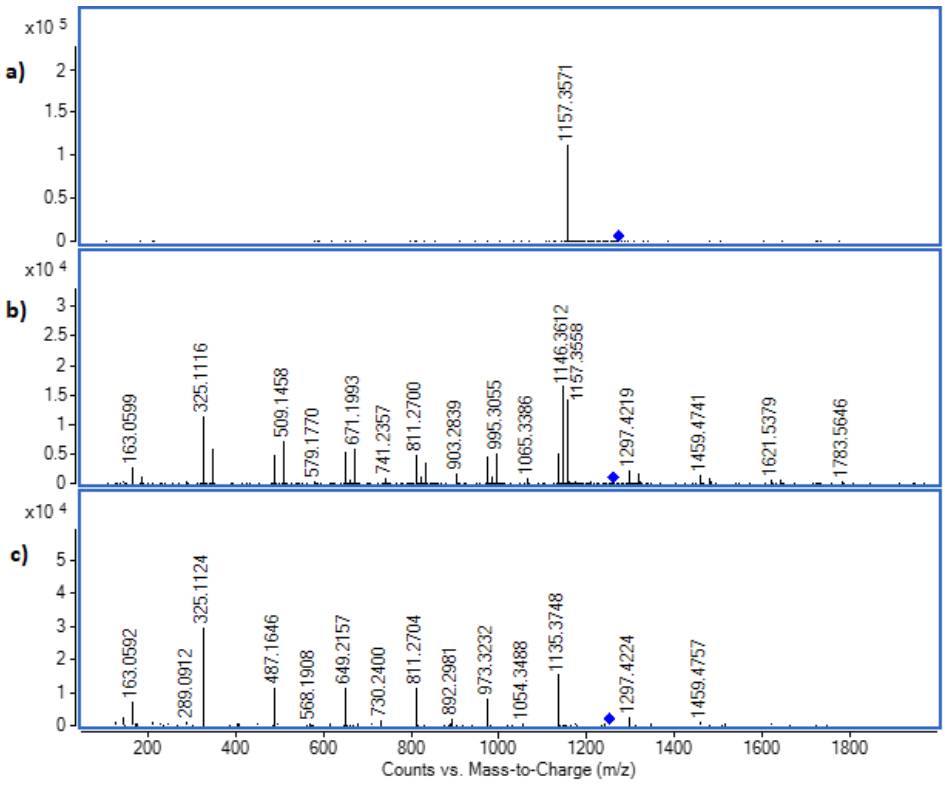

Figure 5. MS/MS spectra of a) $[\text{NAB+2}\beta\text{-CD+2Na}]^{2+}$ (*m/z* 1271.4196), b) $[\text{NAB+2}\beta\text{-CD+Na+H}]^{2+}$ (*m/z* 1260.4285) and c) $[\text{NAB+2}\beta\text{-CD+2H}]^{2+}$ (*m/z* 1249.4374) at 20.0 eV.

3.4. Isothermal microcalorimetric titrations

To gain a more detailed insight into the complexation processes, thermodynamic studies of NAB complexation with β-CDs at 298.15 K in water were performed using isothermal microcalorimetric titrations (Figs. 6a and S11a-S13a). The NAB binding was associated with negative enthalpy changes. Normalized successive enthalpy changes (enthalpy changes divided by the amount of added β-CD) with respect to the β-CD/NAB molar ratio are shown in Figs. 6b and S11b-S13b. The complex stability constant and the reaction enthalpy were processed according to a 1:1 binding model. The standard reaction Gibbs energy and entropy were calculated using fundamental thermodynamic relations [30]. The thermodynamic parameters for the complexation reaction are listed in Table 3. These parameters are crucial in determining

an interaction, as the enthalpy change provides information on the involvement of electrostatic forces, hydrogen bonding, and van der Waals interactions, while the entropy change reveals whether hydrophobic interactions are involved [31,32]. The extent to which each type of force affects the CD-guest interaction has been thoroughly studied and discussed in the literature [33,34]. In general, most CD-guest interactions are enthalpy driven, while entropy can be favorable or unfavorable. As shown in the data presented in Table 1, β-CDs are a moderate binder for NAB, and the stability constants agree well with those calculated from fluorescence measurements. The standard molar enthalpies of complexation are negative for all CDs used. The value of enthalpy is the result of several factors, including the endothermic contribution due to the disruption of hydrogen bonds between the water molecules in the CD cavity, the endothermic dehydration of the included NAB molecule, and the exothermic contribution due to the van der Waals interaction between NAB and the CD cavity. The values of entropies are positive for all CDs studied. They could be explained by desolvation of the embedded part of NAB after inclusion, and from the displacement of water molecules from the cavity. The binding of NAB by CDs is both an enthalpically and entropically favorable process, although the entropic contribution to the reaction Gibbs energy is more dominant for RMβCD and SMβCD. Our data obtained for the NAB/β-CD system agree well with those reported by Todorova et al., for the interaction of β-CD with NAB in phosphate buffer [35].

To investigate the influence of the solvent composition on the thermodynamic parameters, we studied the titration in 5% DMSO-water solution. Unfortunately, we were not able to obtain reproducible data due to the strong background noise [36,37].

Table 3. Thermodynamic parameters for complexation of NAB with cyclodextrins at 25 °C in water.

Macromolecule	$lg\left(\frac{K}{\mathrm{dm^3\ mol^{-1}}}\right) \pm \mathrm{SE}$	$\frac{\Delta_r G^0 \pm \mathrm{SE}}{\mathrm{kJ\ mol^{-1}}}$	$\frac{\Delta_r H^0 \pm \mathrm{SE}}{\mathrm{kJ\ mol^{-1}}}$	$\frac{\Delta_r S^0 \pm \mathrm{SE}}{\mathrm{J\ mol^{-1}\ K^{-1}}}$
β-CD	3.42 ± 0.03	–19.6 ± 0.2	–12.6 ± 0.9	24 ± 3
HPβCD	3.41 ± 0.03	–19.5 ± 0.2	–10.3 ± 0.7	31 ± 3
RMβCD	3.47 ± 0.01	–19.8 ± 0.1	–8.5 ± 0.7	38 ± 2
SBβCD	3.62 ± 0.07	–20.6 ± 0.4	–9.7 ± 0.7	37 ± 4

SE = standard error of the mean (N ≥ 3)

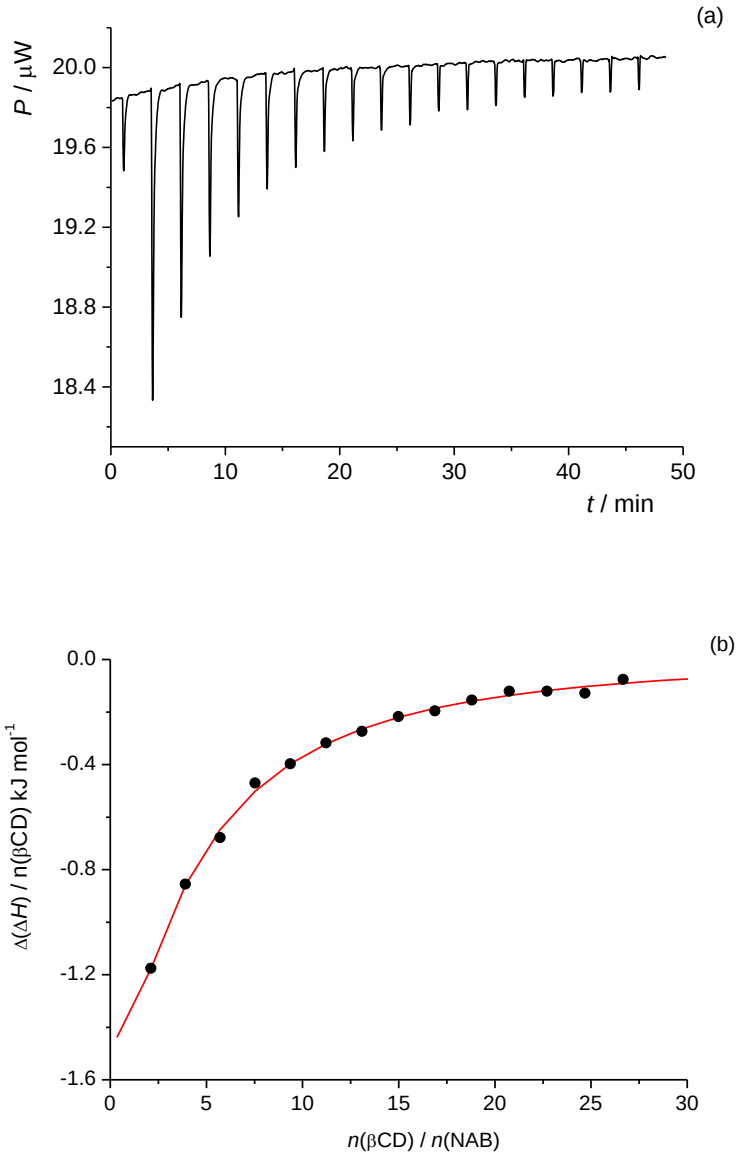

Figure 6. (a) Microcalorimetric titration of NAB (c_0 = 48.9 × 10^{-6} mol L^{-1}, V_0 = 200 μL) with β-CD (c_0 = 8.80 × 10^{-3} mol L^{-1}) in water at 298 K. (b) Dependence of normalized successive enthalpy changes on β-CD/NAB molar ratio. ● experimental; —— calculated.

3.5. *Inclusion mechanism studied by NMR spectroscopy*

3.5.1. Experiments in DMSO-d_6

The analysis of NMR chemical shift perturbations (^{1}H and ^{13}C), intermolecular interactions through space (NOESY), and diffusion coefficients calculations (DOSY) were performed aiming to confirm the complexation and investigate the inclusion mechanism of NAB in the β-

CD cavity. The results indicate that the inclusion in DMSO-d_6 at 25 °C indeed occurs but in a very low percentage. From the DOSY spectra, the calculated complexation was ca. 20 %, which could account for the insignificant chemical shift perturbation observed (Tables S8 and S9) and why the interactions between NAB and β-CD were not seen in the NOESY spectrum (Fig. S32). The reason for such low complexation could be the solvation of NAB by DMSO molecules, or the competition between NAB and solvent molecules for the same interaction sites in the β-CD cavity, both of which can hinder the inclusion.

3.5.2. Experiments in D_2O

Because of the poor solubility of NAB in water, it was not possible to acquire any NMR spectrum other than the proton (with water suppression, Fig. S36). Comparison of this spectrum with the proton spectrum of NAB/β-CD 1:1 complex (Fig. 7) revealed two facts: a) the solubility of the complexed NAB is much higher than that of the free form and b) the chemical shifts of NAB change significantly after the complex is formed, especially 1-H, 5-H and 8-H (Table 4). Both results indicate that the NAB/β-CD complex is formed under the given conditions (D_2O, 25 °C). Moreover, chemical shift comparison between free and bound β-CD (Table 5) revealed the biggest perturbation in 3-H and 5-H, suggesting that the mechanism of complexation is inclusion since these two protons are located on the inner side of the β-CD cavity. All these conclusions are in excellent agreement with the previously reported results [15,16].

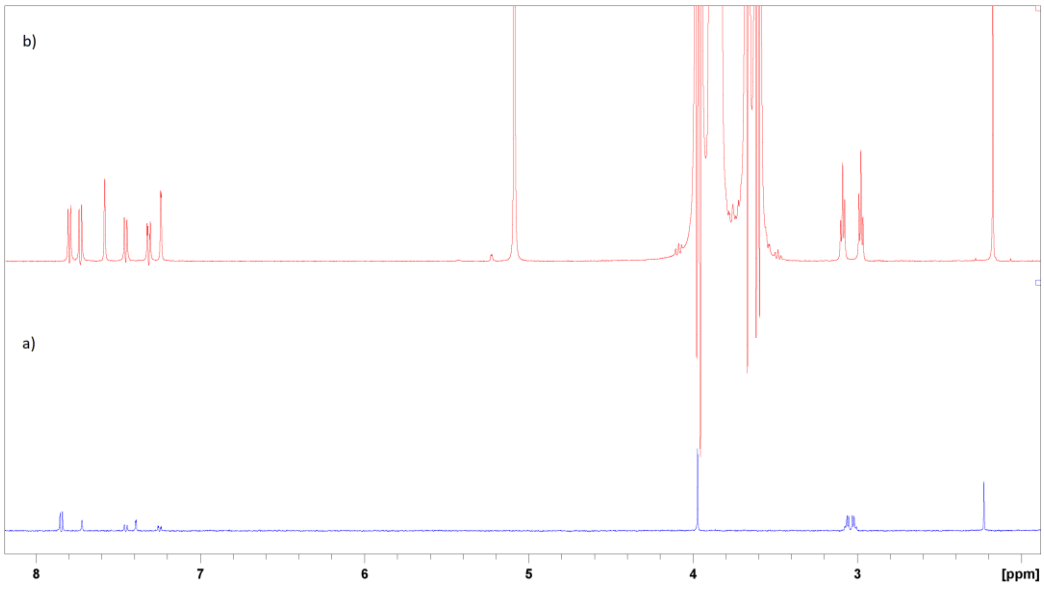

Figure 7. Comparison of proton NMR spectra with WaterGate solvent suppression: a) free NAB and b) NAB/β-CD 1:1 complex, both in D_2O at 25 °C.

Table 4. Comparison of ^{1}H chemical shifts of free NAB and NAB in complex with β-CD, both in D_2O at 25 °C, atoms with biggest differences between free and bound state marked with blue

protons	Δδ (free and bound)	Free nabumetone			Bound nabumetone		
		δ/ppm		*J*/Hz	*δ*/ppm		*J*/Hz
4	–0.051	7.846	d	8.96	7.795	d	9.05
8	–0.118	7.846	d	8.96	7.728	d	9.36
1	–0.139	7.720	s	-	7.581	s	-
3	–0.001	7.454	d	9.10	7.453	dd	1.69; 8.78
7	0.064	7.248	dd	2.70; 9.38	7.312	dd	2.49; 9.24
5	–0.155	7.393	d	2.83	7.238	d	2.44
15	0.013	3.974	s	-	3.987	s	-
11	0.026	3.063	m	-	3.089	t	7.10
12	–0.043	3.019	m	-	2.976	t	7.26
14	–0.054	2.228	s	-	2.174	s	-

Table 5. Comparison of ^{1}H chemical shifts of free β-CD and β-CD in complex with NAB, both in D_2O at 25 °C, atoms with biggest differences between free and bound state marked with blue.

Proton	Δδ (free and bound)	Free β-cyclodextrin			Bound β-cyclodextrin		
		δ/ppm		*J*/Hz	*δ*/ppm		*J*/Hz
1	–0.005	5.091	d	3.46	5.086	d	3.85
3	–0.024	3.989	t	10.08	3.965	t	9.86
6	–0.022	3.901	m	-	3.879	m	-
5	–0.033	3.881	d	2.47	3.848	d	3.74
2	–0.005	3.673	dd	3.58; 10.12	3.668	dd	3.82; 10.30
4	–0.002	3.607	t	9.43	3.605	t	9.57

Our investigation also revealed a large perturbation in the chemical shift of the β-CD 6-CH_2, that has not been reported previously. This difference could be explained by the formation of hydrogen bond between the 6-CH_2OH in β-CD and the carbonyl in NAB, as suggested by Suarez and Diaz in the analysis of their molecular dynamics results [19]. If that is the case, this could be the first obtained experimental data that points toward the 2-butanone substituent is located adjacent to the narrow rim of the β-CD (Fig. 1B).

Intrigued by the possibility of exactly determining which NAB/β-CD conformation is present in the D_2O solution, our study continued by identifying the intermolecular interactions through

space (1D and 2D ROE). Fortunately, the larger solubility of the complex allowed a higher concentration of NAB in the solution, which was a prerequisite for such a study.

Figure 8 shows part of the NAB/β-CD ROESY spectrum with four expected intramolecular NAB interactions (1-H and 3-H with spatially close 2-butanone 11-CH_2 and 12-CH_2), but also a number of intermolecular interactions between NAB and β-CD. In the β-CD cavity, 5-H has interactions with 4-H, 8-H, 1-H, 3-H and probably 5-H from NAB. Similarly, β-CD 3-H, which is also located in the inner cavity of β-CD, has close contact with NAB 4-H, 8-H, 1-H, and 3-H. In other words, 3-H and 5-H of β-CD both show very similar sets of interactions, despite being located at opposite ends of the β-CD cavity. In addition, the 6-CH_2 from the narrow rim of β-CD shows interactions with 7-H and 5-H of NAB, which is evidence for the presence of conformation A in solution.

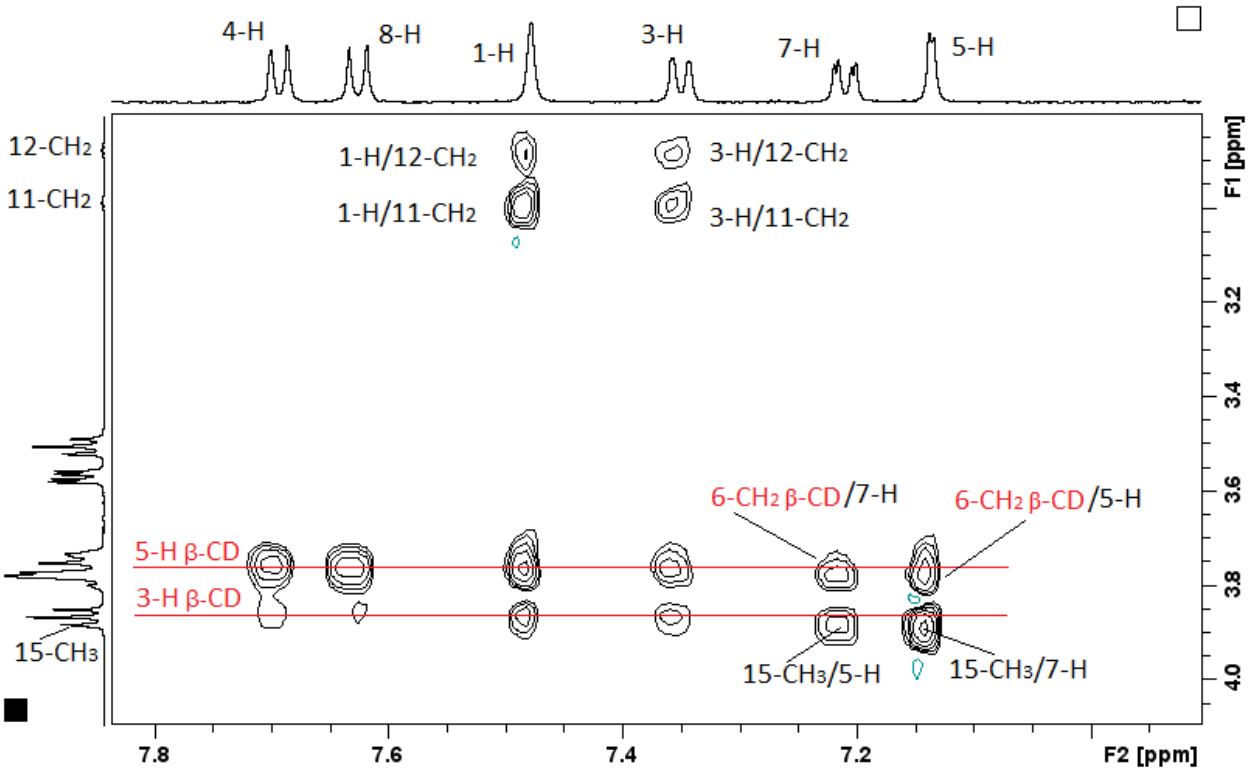

Figure 8. Part of the ROESY spectrum showing intermolecular interactions of NAB with β-CD in 1:1 complex in D_2O at 25 °C

A similar result is seen in the 1D ROE spectra with selective excitation at 3.97 ppm (Fig. 9b). Unfortunately, the selective pulse bandwidth excited both the 3-H β-CD proton (3.97 ppm) along with the NAB 15-CH_3 (3.99 ppm) which resulted in interactions with all the aromatic protons of NAB. Discrimination between these source protons was performed by examination

of the ROESY spectrum: enhancement of 5-H and 7-H were intramolecular from 15-CH_3, and the rest intermolecular from β-CD 3-H.

Figure 9c shows the 1D ROE spectrum with selective excitation at 3.85 ppm, which simultaneously excited both 5-H (3.85 ppm) and 6-CH_2 (3.88 ppm) of β-CD, also resulting in intermolecular interactions with all the aromatic protons in NAB. Although this result did not provide any new information, it confirmed the conclusions from the ROESY experiment.

The appearance of these interactions in the ROE spectra can be explained by the simultaneous presence of both binding orientations in solution, in exchange with free NAB and β-CD. As such, these results represent the first experimental evidence of the equilibrium between both intermolecular orientations in solution and are in agreement with the results of *in silico* methods from the literature.

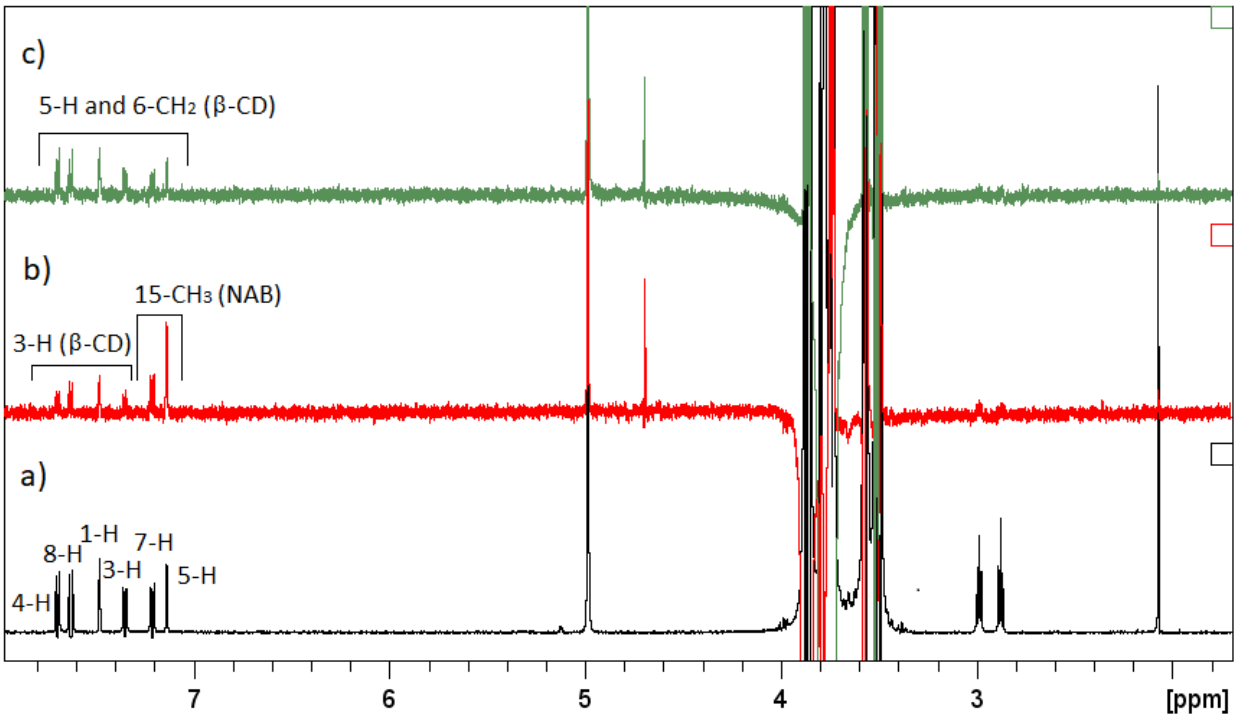

Figure 9. Comparison of a) ^1H, b) 1D ROE with selective excitation at 3.97 ppm (3-H β-CD and NAB 15-CH_3), c) 1D ROE with selective excitation at 3.85 ppm (5-H and 6-CH_2, both β-CD) of NAB/β-CD 1:1 complex in D_2O at 25 °C.

To determine the ratio between free and complexed species in solution, DOSY experiments were performed. In the first step, the diffusion coefficients of free and bound NAB and β-CD

were determined by DOSY. The results are shown in Table 6, while the superposition of the DOSY spectra is shown in Figure 10.

Table 6. Diffusion coefficients (D) calculated from DOSY experiments in D_2O at 25 °C

	D [m^2/s] / 10^{-10}	**Error / 10^{-10}**
Nabumetone - free	6.52	0.07
Nabumetone - bound	2.63	0.08
β-cyclodextrin - free	2.52	0.02
β-cyclodextrin - bound	2.53	0.03

The small difference between free and bound β-CD indicates that its diffusion coefficient was not affected by interaction with NAB. Additionally, the slightly smaller diffusion coefficient of bound NAB compared with bound β-CD can be explained by the fact that a certain percentage of NAB exchanges rapidly between free and bound states. Under these conditions, the equation [38-40] can be used to calculate the percentage of complex formation (p):

$$p = \frac{D_{free} - D_{complex}}{D_{free} - D_{CD}}$$

The percentage of complexation for NAB/β-CD 1:1 complex was calculated to be 97 % in D_2O at 25 °C.

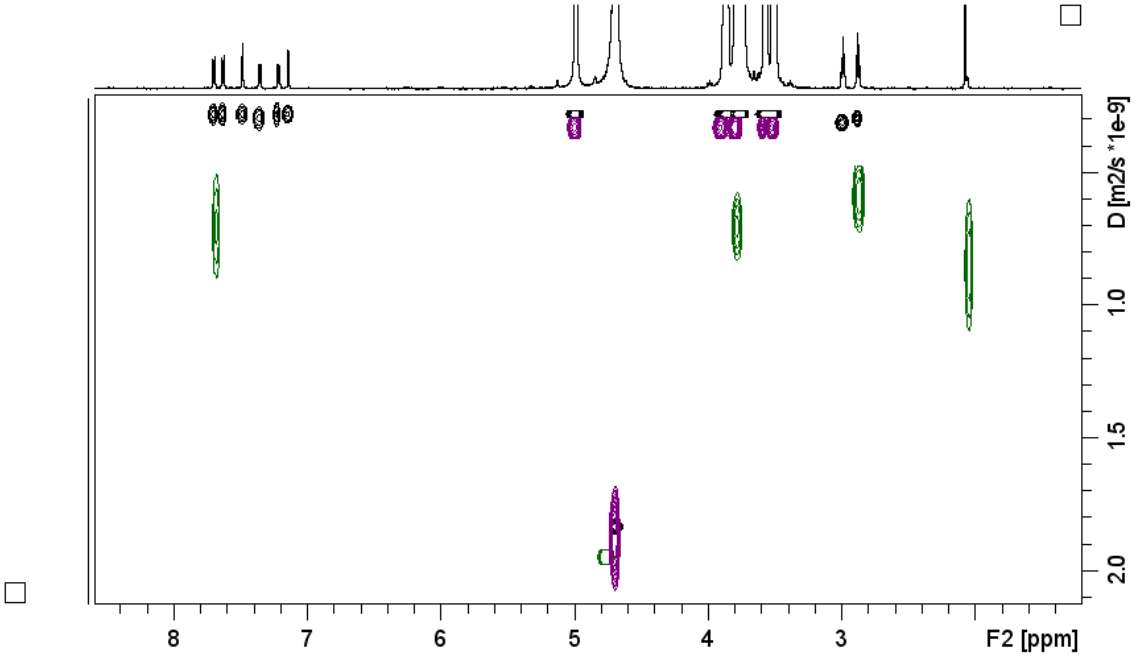

Figure 10. Overlay of DOSY spectra: free NAB (green), free β-CD (purple) and NAB/β-CD 1:1 complex (black) in D_2O at 25 °C.

4. Conclusion

Based on the all results presented, it can be concluded that NAB forms 1:1 inclusion complexes with β-CDs. Increased NAB solubility was achieved up to almost 170 times with SBEβCD at different pH values. The inclusion occurs in both DMSO-d_6 and D_2O at 25 °C. NMR results suggested two possible orientations of NAB in the β-CD cavity and the simultaneous existence of both inclusion orientations (Figure 1) in solution. In both the naphthalene ring sits in the hydrophobic cavity of the β-CD, while the substituents (methoxy and butanone) are oriented toward the edges of the cavity and point toward the solvent. Although this was previously suggested based on *in silico* results, this work presents the first experimental NMR evidence confirming the existence of such an equilibrium in solution.

Conflict of Interest

The authors declare that they have no conflict of interest.

Acknowledgments

This work was supported by the project CIuK (KK.01.1.1.02.0016.) and the project FarmInova (KK.01.1.1.02.0021) co-financed by the Croatian Government and the European Union through the European Regional Development Fund.

Reference

[1] T. Hedner, O. Samulesson, P. Währborg, H. Wadenwik, K.-A. Ung, A. Ekbom, Nabumetone - Therapeutic Use and Safety Profile in the Management of Osteoarthritis and Rheumatoid Arthritis, *Drugs* 64 (2004) 2315–2343. doi: 10.2165/00003495-200464200-00004.

[2] S. M. Kawish, S. Ahmed, A. Gull, M. Aslam, J. Pandit, M. Aqil, Y. Sultana, Development of nabumetone loaded lipid nano-scaffold for the effective oral delivery; optimization, characterization, drug release and pharmacodynamic study, *J. Mol. Liq.* 231 (2017) 514–522. https://doi.org/10.1016/j.molliq.2017.01.107.

[3] A. Matencio, G. Hoti, Y. K. Monfared, A. Rezayat, A. R. Pedrazzo, F. Caldera, F. Trotta, Cyclodextrin Monomers and Polymers for Drug Activity Enhancement, *Polymers* 13 (2021) 1684. https://doi.org/10.3390/polym13111684.

[4] P.C. Pires, M. Rodrigues, G. Alves, A. O. Santos, Strategies to Improve Drug Strength in Nasal Preparations for Brain Delivery of Low Aqueous Solubility Drugs, *Pharmaceutics* 14 (2022) 588. https://doi.org/10.3390/pharmaceutics14030588.

[5] R. Kumar, A. Singh, N. Garg, P.F. Siril, Solid lipid nanoparticles for the controlled delivery of poorly water soluble non-steroidal anti-inflammatory drugs, *Ultrason. Sonochem.* 40 (2018) 686–696. https://doi.org/10.1016/j.ultsonch.2017.08.018.

[6] L. Ferreira, F. Mascarenhas-Melo, S. Rabaça, A. Mathur, A. Sharma, P.S. Giram, K.D. Pawar, A. Rahdar, F. Raza, F. Veiga, P.G. Mazzola, A. C. Paiva-Santos, Cyclodextrin-based dermatological formulations: Dermopharmaceutical and cosmetic applications, *Colloids Surf. B*, 221 (2023) 113012. https://doi.org/10.1016/j.colsurfb.2022.113012.

[7] Q. Wang, A. Zhang, L. Zhu, X. Yang, G. Fang, B. Tang, Cyclodextrin-based ocular drug delivery systems: A comprehensive review, *Coord. Chem. Rev*. 476 (2023) 214919. https://doi.org/10.1016/j.ccr.2022.214919.

[8] M.A. Occhiuzzi, F. Grande, M. De Luca, G. Ragno, A. Garofalo, G. Ioele, Cyclodextrins in topical gel formulation as photoprotective system for Nabumetone, IOP Conf. Series: Materials Science and Engineering, 777 (2020) 012005. doi:10.1088/1757-899X/777/1/012005.

[9] P. Jansook, N. Ogawa, T. Loftsson, Cyclodextrins: structure, physicochemical properties and pharmaceutical applications, *Int. J. Pharm.* 535 (2018) 272–284. https://doi.org/10.1016/j.ijpharm.2017.11.018.

[10] M. Cugovčana, J. Jablan, J. Lovrić, D. Cinčić, N. Galić, M. Jug, Biopharmaceutical characterization of praziquantel cocrystals and cyclodextrin complexes prepared by grinding, *J. Pharm. Biomed. Anal*. 137 (2017) 42–53. http://dx.doi.org/10.1016/j.jpba.2017.01.025.

[11] T. Kezele Špehar, M. Pocrnić, D. Klarić, B. Bertoša, A. Čikoš, M. Jug, J. Padovan, S. Dragojević, N. Galić, Investigation of praziquantel/cyclodextrin inclusion complexation by NMR and LC-HRMS/MS: mechanism, solubility, chemical stability and degradation products, *Mol. Pharm*. **18** (2021) 4210–4223. https://doi.org/10.1021/acs.molpharmaceut.1c00716.

[12] C.V. Pardeshi, R.V. Kothawade, A.R. Markad, S.R. Pardeshi, A.D. Kulkarni, P.J. Chaudhari, M.R.Longhi, N. Dhas, J.B. Naik, S.J. Surana, M.C. García, Sulfobutylether-β-cyclodextrin: A functional biopolymer for drug delivery applications, *Carbohydr. Polym.* 301 (2023) 120347. https://doi.org/10.1016/j.carbpol.2022.120347.

[13] M.E. Davis, M.E. Brewster, Cyclodextrin-based pharmaceutics: past, present and future, *Nat. Rev. Drug Discov.* 3 (2004) 1023–1035. doi:10.1038/nrd1576.

[14] V.J. Stella, R.A. Rajewski, Sulfobutylether-β-cyclodextrin, *Int. J. Pharm.* 583 (2020) 119396. https://doi.org/10.1016/j.ijpharm.2020.119396.

[15] M. Valero, S.M.B. Costa, J.R. Ascenso, M.M. Velázquez, L.J. Rodríguez, Complexation of the Non-steroidal Anti-inflammatory Drug *Nabumetone* with Modified and Unmodified Cyclodextrins, *J. Incl. Phenom. Macrocycl. Chem.* 35 (1999) 663–677. https://doi.org/10.1023/A:1008011228459.

[16] N. Goyenechea, M. Sánchez, I. Vélaz, C. Martin, M.C. Martinez-Ohárriz, G. González-Gaitano, Inclusion complexes of nabumetone with β-cyclodextrins: thermodynamic and molecular modelling studies. Influence of sodium perchlorate, Luminescence, 16 (2001) 117–127. doi: 10.1002/bio.615.

[17] N.A.F. Al-Rawashdeh, Interactions of Nabumetone with *c*-Cyclodextrin Studied by Fluorescence Measurements, *J. Incl. Phenom. Macrocycl. Chem.* 51 (2005) 27–32. https://doi.org/10.1007/s10847-004-1502-9.

[18] W. Chen, C.-E. Chang, M.K. Gilson, Calculation of Cyclodextrin Binding Affinities: Energy, Entropy, and Implications for Drug Design, *Biophys. J.* 87 (2004) 3035–3049. https://doi.org/10.1529/biophysj.104.049494.

[19] D. Suárez, N. Dıáz, Conformational and entropy analyses of extended molecular dynamics simulations of α-, β- and γ-cyclodextrins and of the β-cyclodextrin/nabumetone complex, *Phys. Chem. Chem. Phys.* 19 (2017) 1431–1440. https://doi.org/10.1039/C6CP06107A.

[20] N. Bensouilah, B. Boutemeur‐Kheddis, H. Bensouilah, I. Meddour, M. Abdaoui, Host-guest complex of nabumetone: β-cyclodextrin: quantum chemical study and QTAIM analysis, *J. Incl. Phenom. Macrocycl. Chem*. 87 (2017) 191–206. https://doi.org/10.1007/s10847-016-0690-4.

[21] A. Jerschow, N. Müller, 3D Diffusion-Ordered TOCSY for Slowly Diffusing Molecules, *J. Magn. Reson. A* 123 (1996) 222–225. doi.org/10.1006/jm re.1997.1123

[22] A. Jerschow, N. Müller, Suppression of Convection Artifacts in Stimulated-Echo Diffusion Experiments. Double-Stimulated-Echo Experiments. *J. Magn. Reson*. 1997, 125 (2), 372–375. doi.org/10.1006/jmre.1997.1123

[23] T. Higuchi, K.A. Connors, Phase-Solubility Techniques. In *Advances in Analytical Chemistry and Instrumentation*; Reilley, C. N., Ed.; Wiley-Interscience, NewYork, 1965; pp 117–212.

[24] European Pharmacopoeia Commission. *European Pharmacopoeia*, 10th ed., Council of Europe: Strasbourg, France, 2019., pp. 188 – 191.

[25] N. Goyenechea, M. Sánchez, I. Vélaz, C. Martin, C. Martinez-Ohárriz, A. Zornoza, Interactions of Nabumetone with Cyclodextrins in Solution and in the Solid State, *J. Incl. Phenom. Macrocycl. Chem*. 44 (2002) 283–287. https://doi.org/10.1023/A:1023016114329.

[26] M. Kfoury, D. Landy, S. Fourmentin, Characterization of Cyclodextrin/Volatile Inclusion Complexes: A Review, *Molecules*, 23 (2018) 1204. doi:10.3390/molecules23051204.

[27] N.S. Kim, S.H Moon, H.S. Choi, J.H. Lee, S. Park, H. Kang, Simultaneous separation and determination of 20 potential adulterant antigout and antiosteoporosis pharmaceutical compounds in herbal food products using LC with electrospray ionization MS/MS and LC with quadrupole-time-of-flight MS, *J. Sep. Sci*. 43 (2020) 2750–2765. doi: 10.1002/jssc.201901204.

[28] M. Valero, J. Tejedor, L.J. Rodríguez, Encapsulation of nabumetone by means of -drug: (β-cyclodextrin)2:polyvinylpyrrolidone ternary complex formation, *J. Lumin*. 126 (2007) 297–302. https://doi.org/10.1016/j.jlumin.2006.07.028.

[29] P.S. Bruni, S. Schürch, Fragmentation mechanisms of protonated cyclodextrins in tandem mass spectrometry, *Carbohydr. Res*. 504 (2021) 108316.

https://doi.org/10.1016/j.carres.2021.108316.

[30] J.E. Ladbury, Calorimetry as a tool for understanding biomolecular interactions and an aid to drug design, *Biochem. Soc. Trans*. **38** (2010) 888–893. https://doi.org/10.1042/BST0380888.

[31] A. Cooper, C.M. Johnson, J.H. Lakey, M. Nöllmann, Heat does not come in different colours: entropy–enthalpy compensation, free energy windows, quantum confinement, pressure perturbation calorimetry, solvation and the multiple causes of heat capacity effects in biomolecular interactions, *Biophys. Chem*. **93** (2001) 215–230. https://doi.org/10.1016/S0301-4622(01)00222-8.

[32] M.V. Rekharsky, Y. Inoue, Microcalorimetry, in: Dodziuk, H. (Ed.), Cyclodextrins and Their Complexes. Wiley-VCH Verlag GmbH & Co. KGaA, Weinheim, FRG, 2006. pp. 199–230. https://doi.org/10.1002/3527608982.ch8.

[33] L. Liu, Q.-X. Guo, The Driving Forces in the Inclusion Complexation of Cyclodextrins, *J. Incl. Phenom. Macrocycl. Chem*. **42** (2002) 1–14. https://doi.org/10.1023/A:1014520830813.

[34] M.V. Rekharsky, Y. Inoue, Complexation Thermodynamics of Cyclodextrins. *Chem. Rev*. **98** (1998) 1875–1918. https://doi.org/10.1021/cr970015o.

[35] N.A. Todorova, F.P. Schwarz, The role of water in the thermodynamics of drug binding to cyclodextrin, *J. Chem. Thermodyns*. **39** (2007)1038–1048. doi:10.1016/j.jct.2006.12.019.

[36] C. Senac, S. Desgranges, C. Contino-Pépin, W. Urbach, P.F.J. Fuchs, N. Taulier, Effect of Dimethyl Sulfoxide on the Binding of 1-Adamantane Carboxylic Acid to β- and γ-Cyclodextrins, *ACS Omega*. **3** (2018) 1014–1021. doi:10.1021/acsomega.7b01212.

[37] K. Fotiadou, A. Thanassoulas, G. Nounesis, K. Yannakopoulou, Cooperative heterodimer formation between per-guadinylated and carboxylated or phosphorylated cyclodextrins in DMSO and DMSO–water studied by NMR spectroscopy and microcalorimetry, *Supramol. Chem.* **23** (2011) 493–500. doi:10.1080/10610278.2010.550918.

[38] R. Rymdén, J. Carlfors, P. Stilbs, Substrate Binding to Cyclodextrins in Aqueous Solution: A Multicomponent Self-Diffusion Study. *J. Incl. Phenom.* 1 (1983) 159–167. https://doi.org/10.1007/BF00656818.

[39] M. Lin, D.A. Jayawickrama, R.A. Rose, J.A. DelViscio, C.K. Larive, Nuclear Magnetic Resonance Spectroscopic Analysis of the Selective Complexation of the Cis and Trans Isomers of Phenylalanylproline by β-Cyclodextrin. *Anal. Chim. Acta* **307** (1995) 449–457. https://doi.org/10.1016/0003-2670(95)00006-L.

[40] A. Calderini, F.B.T. Pessine, Synthesis and Characterization of Inclusion Complex of the Vasodilator Drug Minoxidil with β-Cyclodextrin. *J. Incl. Phenom. Macrocycl. Chem.* **60** (2008) 369–377. https://doi.org/10.1007/s10847-007-9387-z.

Declaration of interests

☒The authors declare that they have no known competing financial interests or personal relationships that could have appeared to influence the work reported in this paper.

☐The authors declare the following financial interests/personal relationships which may be considered as potential competing interests:

Click here to access/download
Supplementary Material
Supporting Information.docx